Study of UV-Vis absorption spectra of magnetic molecule tripyridinium bis[tetrabromidoferrate(III)] bromide with density functional formalisms

F. Baniasadi[1], M. B. Fathi[2,*], M. M. Tehranchi[1], V. Amani[3]

[1]*Physics Department, Shahid Beheshti University, Tehran, Iran*
[2,*]*Condensed Matter Department, Faculty of Physics, Kharazmi University, Tehran, Iran*
[3]*Department of Chemistry, Farhangian University, Tehran, Iran*
[*]Corr. Auth. email: fathi@khu.ac.ir; mb.fathi@gmail.com, Mobile phone: +989128391426

Abstract

The UV-Vis absorption spectra of the discrete magnetic molecules $[py.H]_3[FeBr_4]_2Br$ were calculated based on density functional theory with B3LYP exchange-correlation functional in acetonitrile solution. The molecule was dissolved dilutely in acetonitrile to ensure that its experimental response can be attributed to a single dispersed molecule without significant interaction to other molecules. The experimental UV-Vis absorption spectra show four typical peaks in UV region and three peaks in visible region. A number of different basis sets are employed to compare the experimental data with the theoretical absorption spectra on different levels of basis sets. The comparison of experimental data with theoretical computation shows that choosing 6-311++G** improves computational results mainly in visible region and makes little differences between results based on DFT and TDDFT in other wavelength domains, especially in UV wavelengths. The simulated results are of importance in simulating the response of these molecular magnets as a discrete asymmetric unit to applied light.

Keyword: Molecular magnet, DFT, TDDFT, UV-Vis absorption spectra.

PACS numbers: 78.40.−q; 75.50.−y; 71.15.Mb; 82.90.+j.

1. Introduction

Study of electronic structure of molecular magnets (MM) has become a noticeable research trend owing to their interesting magneto-optical, electro-optical and photo-magnetic properties [1-6]. In an effort to interpreting the complete map of their electronic structure, a variety of experimental and theoretical methods are proposed [7-10]. Experimentally, the electronic structures of molecules are generally elucidated using the transition and absorption spectra [11-12]. The ultraviolet-visible (UV-Vis) absorption, ultraviolet photoelectron spectroscopy (UPS) and energy loss spectroscopy (ELS) are the almost identical methods usually justified by theoretical calculations to determine the inherent electronic structure of molecular systems [12-13].

The experimental spectroscopic data are mostly simulated by means of quantum chemistry calculations such as Hartree-Fock configuration interaction single (RHF/CIS) [14], time-dependent density functional theory (TDDFT) [14-16] and certain semi-empirical calculations

via INDO or CNDO Hamiltonian [14]. Among them, TDDFT has become widespread and popular technique to reproduce experimental spectroscopic results. This method is designed to yield the exact excited state (ES) by means of developing the ground state (GS) with DFT formalism considering that the potentials and densities of a many-body system vary with time [13]. TDDFT alongside with high-level basis sets is able to approximate the electronic transitions with a good degree of accuracy and low computational time cost [16].

The present study aims at deeper understanding of ultraviolet and visible spectra (UV-Vis) of tripyridinium bis[tetrabromidoferrate(III)] bromide molecular magnet. Despite many theoretical attempts for electronic structure calculation of materials, the problem of finding the better approximate basis sets for simulation of MMs challenges condensed matter researchers. The line-width of absorption spectra is of critical importance for completion of simulation, even at the first-principles level. For this purpose, we simulate the molecular magnet of chemical formula $[py.H]_3[FeBr_4]_2Br$ via density functional approximation scheme, and examine the proficiency of these methods to determine the energy levels for predicting electronic transition in this complex in some wavelengths regions. This MM has been the subject of intense researches since the development of a new generation of electronic devices [17-20]. Therefore, identification of electronic transitions in these molecular complexes was a great characterization problem since then.

This work is organized as follows: Next section is devoted to the theoretical method used for estimating absorption spectrum. Section III is dedicated to computational details obtained via Gaussian 2003 (A.B.3) [21-23] and Gausssum 2.2 [24]. Then, the comparison of computational results with the experimental data is presented. Summary and discussion of the results are presented at the end.

2. Theoretical formulation of absorption spectra

The absorption of light by the chemical species can be attributed to electronic transitions. These transitions are associated to the changes in energy between the states corresponding to the frequency variations ν, wavelength λ and wave number of photons absorbed $\nu'(\equiv \nu)$. The absorption of light by compounds in solution is described by Bear-Lambert law [24, 25].

Experimentally, participation of each energy level in electronic transitions can be evaluated by integration on all energies in interval corresponding to the line-width, via the dimensionless oscillator strength (f) for electronic transition. From the viewpoint of the transition dipole approximation, oscillator strength is estimated through electric dipole transition $(P_{i\to f})$ between initial i and final state f [26, 27]:

$$f = \frac{2m_{\mathrm{e}}}{3\hbar \mathrm{e}^2}\,\Delta\omega_{i\to f}\left|P_{i\to f}\right|^2 \qquad (1)$$

where, all symbols are famous. Oscillator strength can be calculated using Gaussian function $g(x) = N.\mathrm{e}^{-\alpha(x-\beta)^2}$ with the normalization constant N on the center of β, for approximating the ε line-shape, by integrating over the whole energy space. Employing the relation between α

exponent and full width at half maximum (FWHM), $\Delta_{1/2}\nu = \sqrt{\frac{4\ln 2}{\alpha}}$ and $\beta = \nu_{i\to f}$, the molar absorption coefficient is obtained [28],

$$\varepsilon(\nu) = \frac{2.175\times 10^{8}\left(\mathrm{L.mol^{-1}.cm^{-2}}\right)}{\Delta_{1/2}\nu} f \exp\left[-2.772(\frac{\nu-\nu_{i\to f}}{\Delta_{1/2}\nu})\right]. \quad (2)$$

To compute f and $\nu_{i\to f}$ it is required to provide the excited states. The formalism of TDDFT is popular to find time variant dynamical quantities, such as excitation energies and frequency-oriented response properties in the presence of any dynamical potentials (electric, magnetic fields or light) [16]. In this model, the classical optical light field (electric field $\vec{E}(t)$) couples to dipole moment of atom causing to time-dependent wave function ($\psi(\mathbf{r},t)$). This wave function can be written as liner combination of the stationary eigenfunctions, $\psi_n(\mathbf{r})$ [28].

With employing time dependent perturbation theory with linear response theory, the wave function can be obtained as

$$\psi(\mathbf{r},t) = \mathrm{e}^{-i\varepsilon_m t}[\psi_m(\mathbf{r}) - \sum_{n\neq m}\frac{\left|\mathbf{p_{mn}}\right|}{\hbar}\psi_m(\mathbf{r})\int\frac{\mathrm{d}\omega}{2\pi}\frac{E(\omega)\mathrm{e}^{-i\omega t}}{\omega+\varepsilon_{mn}+i\gamma} \quad (3)$$

where, $\mathbf{p}_{mn}$ is the electric dipole matrix element in dipole transition approximation. The field-induced polarization, $P(t)$, is thus given by,

$$\begin{aligned} P(t) &= -n_0\sum_{n\neq m}\frac{\left|\mathbf{p_{mn}}\right|^2}{\hbar}\int\frac{\mathrm{d}\omega}{2\pi}E(\omega)\mathrm{e}^{-i\omega t}[\frac{1}{\omega+\varepsilon_{mn}+i\gamma}-\frac{1}{\omega-\varepsilon_{mn}+i\gamma}], \\ &= \int\frac{\mathrm{d}\omega}{2\pi}P(\omega)\mathrm{e}^{-i\omega t}. \end{aligned} \quad (4)$$

Since, the frequency dependent polarization, $P(\omega)$, depends on the electric field through $P(\omega)=\chi(\omega)E(\omega)$, the optical susceptibility, $\chi(\omega)$, can finally be evaluated.

The absorption coefficient $\alpha(\omega)$ can be determined by imaginary part of $\chi(\omega)$ as [20]

$$\alpha(\omega) = \frac{4\pi}{n(\omega)c}\chi''(\omega) \quad (5)$$

where, $n(\omega)$ is [20]

$$n(\omega) = \sqrt{\frac{1}{2}}\left\{1+4\pi\chi'(\omega)+\sqrt{\left[1+4\pi\chi'(\omega)\right]^2+\left[4\pi\chi''(\omega)\right]^2}\right\}^{1/2}. \quad (6)$$

To estimate the absorption coefficient in a comp

lex containing many atoms, contribution of each atom should be taken into account via molecular orbitals and their expansion coefficients [29, 30, 31]. Owning to lack of any exact solution for calculation of wave function in many body systems, various approximations employ different sets of mathematical wave functions. Molecular orbitals are nothing other than linear combination of atomic orbitals (LCAO) [32],

$$\psi_i = \sum_{\mu=1}^{n} c_{\mu i}\varphi_\mu \quad (7)$$

where, $c_{\mu i}$ and φ_μ are the expansion coefficients and μ^{th} atomic orbital, respectively. In Gaussian format, φ_μ is

$$\varphi_\mu = \sum_{j=1}^{p} d_{\mu j} N_g (x - x_A)^a (y - y_A)^b (z - z_Z)^c \exp(-\alpha[(x - x_A) + (y - y_A) + (z - z_Z)]) \quad (8)$$

where, α is the exponent, $d_{\mu j}$ is atomic expansion coefficient, $r_A(x_A, y_A, z_A)$ is position of atom A, a, b and c are integral exponents which are associated to angular momentum via $L = a + b + c$.

3. Results and Discussion

All calculations are performed making use of the computational cluster SARMAD in Shahid Beheshti University. At least, 64 cores are used during the calculational processes for various different codes with different basis sets and potentials.

3.1 Tripyridinium bis[tetrabromidoferrate(III)]bromide

The formula for the molecule under study is $[py.H]_3[FeBr_4]_2Br$, which belongs to the iron tetrahaloferrate(III) group. This complex was first synthetized by Robin *et al.* [17]. In our previous work, we reported the abundant molecular structure of $[py.H]_3[FeBr_4]_2Br$ in acetonitrile solvent, characterized by Debye function analysis of experimental X-ray intensities [33]. The structure has been optimized previously by DFT in scheme of B3LYP and 6-31g* approximation and the optimized structure is reproduced in Fig. 1 (figure from [33]).

Figure 1 The plausible abundant molecular structure of $[py.H]_3[FeBr_4]_2Br$ complex in acetonitrile [33].

3.2 Ground state energy levels

Owing to relation between the energy difference of highest occupied molecular orbital (HOMO) and lowest unoccupied molecular orbital (LUMO) $E = E_{LUMO} - E_{HOMO}$, with the absorption energy $h\nu_{i\to f}$, the ground state energies are calculated. All calculations were done by considering acetonitrile solvent as the media (making use of IEFPCM keyword). The DFT method with various different potentials is applied with several levels of Pople-type basis sets with or without diffuse and polarized functions. Those approximations are itemized according to the split valence basis set and diffuse function as: 6-31G, 6-31G*, 6-31G **, 6-31+G, 6-31+G*, 6-31+G **, 6-31++G, 6-31++G*, 6-31++G **, 6-311G, 6-311G*, 6-311G **, 6-311+G, 6-311+G*, 6-311+G **, 6-311++G, 6-311++G*, 6-311++G **. All calculations are carried out with Gaussian 2003 (A.B.3) [14]. In Tab. 1, the ground state energy for different approximations in atomic unit $(1\mathrm{Hartree}{=}27.21\mathrm{eV})$ are listed.

Table 1 Ground state energy of the molecule at different Pople basis sets in atomic units.

Referring to Tab. 1, calculated energies associated with 6-31+G**, 6-31++G**, 6-311+G** and 6-311++G** were less than other calculations. These approximations will be employed later.

3.3 Density of states

Density of states (DOS) can be utilized as a valuable tool to realize transition rate or absorption spectrum. DOS demonstrates the number of states in a certain energy difference or in a given energy interval. The DOS of isolated molecule is defined as a function of single particle energy eigenvalue (ξ),

$$\mathrm{DOS} = \sum_i \delta(E - \xi_i) \tag{9}$$

The DOS simply takes into account Gaussian broadening function [34]. This quantity for different double-zeta and triple-zeta basis sets, calculated using Gausssum [23] with FWHM=0.2eV, are shown in Figs. 2 and 3.

Figure 2 Calculated DOS by Double-zeta Basis Sets: 6-31+G** and 6-31++G**.

Figure 3 Calculated DOS using Triple-zeta Basis Sets: 6-311+G** and 6-311++G**.

3.4 TDDFT simulation of absorption spectrum

The variation of MOs' energies and DOSs at different basis set levels, appear that they poses similar features with some difference. These differences, one of which at the Fermi surface, reflects some remarks about the adaption of basis set or approximation chosen for simulations. Based on the ground state energies (Table 2), we choose 6-31++G** from the first column and 6-311++G** from the second column, since they both yield the lowest ground state energy for the molecule in their categories.

DOS results, also, represent some illuminating guide about the well-suited basis set for further simulations. The experimental absorption spectrum versus wave-length is shown in Fig. 9. Two peaks appear at wave-lengths about $\lambda = 470, 390 \ \mathrm{nm}$, which are equivalent to energies $\varepsilon \simeq 2.64, 3.2 \ \mathrm{eV}$. If we choose, in Koopman's single particle picture, two corresponding electronic transitions from the Fermi level, DOSs in Figs. 2 and 3 show that 6-311++G** and 6-31++G** fill the Fermi level (shown by arrows), which permits electron to transit to higher levels; this can show us the most well-suited basis sets for molecule's simulation. In addition, as a *rough* estimate of the transition energies, these two DOSs simulated by the mentioned basis sets allow transitions nearly equivalent to energies in the absorption peaks, as shown by arrows.

Therefore, two basis sets 6-31++G** and 6-311++G** are applied as a benchmark for the next calculations in TDDFT studies. TDDFT calculations were performed making use of G03 and the UV-Vis absorption spectra for the mentioned basis sets. The results are plotted via Gausssum package using different FWHM values (0.1, 0.2, 0.3 eV) in Fig. 4.

Figure 4 TDDFT simulation of absorption spectra using different FWHM values (0.1, 0.2 and 0.3 eV).

3.5 DFT calculations employing different levels of approximation

Referring to the minimum ground state energy in Table 1, two 6-31++G** and 6-311++G** basis sets are adapted for a comparative study between DFT and TDDFT, and calculating electronic spectra and absorption spectrum. We find the exponents and coefficients for the atomic orbitals and then the molecular orbitals. The exponents and coefficients are obtained via

single point calculation in DFT and B3LYP by means of pop=full and gf print keywords. Using the outputs of calculations for the mentioned basis set, the molecular orbitals are evaluated. Fig. 5 demonstrates the probability of finding electrons in some of these MOs.

Figure 5 The probability of finding electrons in H-2, H-1, H, L, L+1, L+2.

Having the MOs for the UV-Vis transitions, the related dipole transition matrix elements P_{nm} can be estimated. Calculations were well carried out by means of Monte Carlo integration with errors less than ~6%. Results for some selected transitions (HOMOs to LUMO) via two 6-31++G** and 6-311++G** basis sets are tabulated in Table 2.

Table 2 Selected transition dipole matrix elements by 6-31++G** and 6-311++G** basis sets.

The MOs related to the transitions in Tab. 2 for $6\text{-}31{+}{+}\mathrm{G}^{**}$ and $6\text{-}311{+}{+}\mathrm{G}^{**}$ basis sets are shown in Figs. 6 and 7, respectively.

Figure 6 Selected HOMO and LUMOs using $6\text{-}31{+}{+}\mathrm{G}^{**}$.

Figure 7 Selected HOMO and LUMOs using $6\text{-}311{+}{+}\mathrm{G}^{**}$.

As can be seen from the MOs in ground states (H-2, H-1 and H) and excited states (L, L+1 and L+2) in both 6-31++G** and 6-311++G** basis sets (Figs. 6&7), the role of pyridinium rings in absorption for the wavelengths which are assumed in Table 2 can be neglected.

3.6 The refractive index

After calculation of all probable P_{nm} for transitions in the range of 300-800 nm wavelength, the refractive index $n(\omega)$ can now be calculated using the relations (4-6) making use of different line-widths, $\gamma = 0.1, 0.2, 0.3\mathrm{eV}$. The results of computations are depicted in Fig. 8.

Figure 8 The refractive indexes at the different line-widths (0.1. 0.2 and 0.3 eV).

The appearance of the refractive indexes seems to have special effect on the diagram of $\chi(\omega)$, and causes major differences in the absorption curve. The main variations appear in the magnitude of $n(\omega)$ and using different line-widths reveals the finer structures in the curve, so that the line-width $\gamma = 0.1\mathrm{eV}$ reveals better the peaks and valleys. Knowing the refractive index is crucial for calculation of absorption coefficient, which will be done in the last subsection (vide infra).

3.7 The absorption coefficient

The final step is the calculation of absorption coefficient $\alpha(\omega)$. The results of these calculations will help us to compare theoretical data with that of experiment and to choose the well-suited basis set for approximating the experimental absorption spectrum for

$[py.H]_3[FeBr_4]_2Br$ complex, measured in acetonitrile solvent. Fig. 9 shows the theoretical absorption spectra alongside with the experimental data.

Figure 9 DFT simulation of absorption spectra at different line-widths (0.1. 0.2 and 0.3 eV) are compared with that of experiment.

With regard to Fig. 9, both basis sets have identical consequences in outside 500-800 nm while the size of peaks in the range of 300-600 nm are significantly different with each other. The experimental absorption spectrum for complex of $[py.H]_3[FeBr_4]_2Br$ is measured in acetonitrile solvent. The theoretical calculations provide mostly the peaks but the places of peaks are shifted to larger wavelengths (smaller energies). These especial features of theoretical curves rely on the basics of disabilities of DFT to recover the energies of excited states. The height of peaks and valleys are comparable more suitably than the places of energies, since the oscillator strengths calculated for estimating dipole moment matrix is reliable yet in DFT scheme. In fact, the single excited electron transfer doesn't yield the very complicated picture of many-body correlative system, in which all electrons may be excited due to a single photon irradiation.

4. Summary and conclusion

The experimental absorption spectrum of the magnetic molecule tripyridinium bis[tetrabromidoferrate(III)] bromide is simulated within the scheme of density functional formalisms to decide on the best fitting procedure for simulating the experimental results, making use of TDDFT and DFT. As a conclusion, choosing TDDFT can determine the place of peaks in wave-length region more accurate than choosing DFT, but can't fully estimate the strength of peaks in comparison to DFT. On the other hand, choosing DFT can better determine the height of peaks (*i.e.*, the strengths of peaks). In addition, the theoretical results are fitted to that of experiment with the most plausible line-width of the molecule about 0.1 eV.

The deviation in theoretical absorption spectra from the experimental may be attributed to: 1. neglecting pyridinium rings in HOMOs and LUMOs; 2. The abilities of DFT in determining the excited states and 3. The faulty picture of single electron excited in the process of irradiation of matter with a single photon (in fact, if the measurement can be done by a single electron transfer, such as in the PES or ARPES experiments, the measurement will yield more fittable results by DFT). So, considering the single excited MOs in the electron transitions, may correct the energies of levels by an exciton-like transition, which includes electron-hole Columbic interaction.

References

[1] Ohkoshi, S-i, Hashimoto, K. "Photo-magnetic and magneto-optical effects of functionalized metal polycyanides", **2**, 1, 71-88 (2001).

[2] Xu, Y-K., Li, H., He, B-G. *et al.* "Electronic Structure and Magnetic Anisotropy of Single-Layer Rare-Earth Oxybromide", *ACS Omega* **5**, 23, 14194-14201 (2020).

[3] Gong, C., Li, L., Li, Z. *et al.* "Discovery of intrinsic ferromagnetism in two-dimensional van der Waals crystals". *Nature* **546**, 265- 269 (2017).
[4] Sieklucka, B. and Pinkowicz, D. Eds., *Molecular Magnetic Materials: Concepts and Applications*, (Wiley, 2017).
[5] Boukhvalov, D. W., Al-Saqer, M., Kurmaev, E. Z. *et al.* "Electronic structure of a Mn_{12} molecular magnet: Theory and experiment" *Phys. Rev. B* **75**, 014419 (2007).
[6] Carlotto, S., Sambi, M., Sedona, F. *et al.* "A Theoretical Study of the Occupied and Unoccupied Electronic Structure of High- and Intermediate-Spin Transition Metal Phthalocyaninato (Pc) Complexes: VPc, CrPc, MnPc, and FePc. *Nanomaterials* **11**, 54 (2021).
[7] Xue, Z. X., Qua, Y., Zan, Y. H. *et al.* "Broadening of the optical absorption spectra in ZnO nanowires induced by mixed-phase $Mg_xZn_{1-x}O$ shells" *Journal of Applied Physics* **129**, 024502 (2021).
[8] Wang, H., Li, J., Li, K. *et al.* "Transition metal nitrides for electrochemical energy applications" *Chem. Soc. Rev*., **50**, 1354-1390 (2021).
[9] Verdaguer, M. "Rational synthesis of molecular magnetic materials: a tribute to Olivier Kahn" *Polyhedron* **20** 1115 (2001).
[10] Garino, C., Borfecchia, E., Gobetto, R. *et al.* "Determination of the electronic and structural configuration of coordination compounds by synchrotron-radiation techniques" *Coord. Chem. Rev*. **277–278**, 130-186 (2014).
[11] Anak, B., Bencharif, M. and Rabilloud, F. "Time-dependent density functional study of UV-visible absorption spectra of small noble metal clusters (Cu_n, Ag_n, Au_n, n = 2–9, 20)" *RSC Adv*. **4** 13001-13011 (2014).
[12] Pal, G., Pavlyukh, Y., Hübner, W. *et al.* "Optical absorption spectra of finite systems from a conserving Bethe-Salpeter equation approach" *EPJ B* **79**, 327-334 (2011).
[13] Dreuw, A. and Head-Gordon, M. "Single-Reference ab Initio Methods for the Calculation of Excited States of Large Molecules" *Chem. Rev.* **105** 4009-4037 (2005).
[14] Runge, E., Gross, E. K. U. "Density-Functional Theory for Time-Dependent Systems" *Phys. Rev. Lett.* **52** 997 (1984).
[15] Rohringer, N., Peter, S. and Burgdorfer, J. "Calculating state-to-state transition probabilities within time-dependent density-functional theory" *Phys. Rev. A* **74** 042512, 1 (2006).
[16] Anouar, E. H., Osman, C. P., Frederic, J. *et al.* "UV/Visible spectra of a series of natural and synthesised anthraquinones: experimental and quantum chemical approaches" *SpringerPlus* **3** 233, 1 (2014).
[17] a) Ginsberg, A. P. and Robin, M. B. "The Structure, Spectra, and Magnetic Properties of Certain Iron Halide Complexes" *Inorg. Chem.* **2** (4) 817-822 (1963). b) Zora, J. A., Seddon, K. R., Hitchcock, P. B. *et al*. "Magnetochemistry of the tetrahaloferrate(III) ions. 1. Crystal structure and magnetic ordering in bis[4-chloropyridinium tetrachloroferrate(III)]-4-chloropyridinium chloride and bis[4-bromopyridinium) tetrachloroferrate(III)]-4-bromopyridinium chloride" *Inorg. Chem.* **29** (18) 3302-3308 (1990). c) Lowe, C. B., Carlin, R. L., Schultz, A. J. *et al*. "Magnetochemistry of the tetrahaloferrate(III) ions. 2. Crystal structure and magnetic ordering in [4-Br(py)H]3Fe2Cl1.3Br7.7 and [4-Cl(py)H]3Fe2Br9. The superexchange paths in the A3Fe2X9 salts" *Inorg. Chem.* **29** (18) 3308-3315 (1990). d) Lowe, C. B., Schultz, A. J., Shaviv, R. *et al.* "Magnetochemistry of the Tetrahaloferrate(III) Ions. 7. Crystal Structure and Magnetic Ordering in (pyridinium)3Fe2Br9" *Inorg. Chem.* **33** (14) 3051 (1994).
[18] Baniasadi, F., Tehranchi, M. M., Fathi, M. B. *et al*. "Intra-molecular magnetic exchange interaction in the tripyridinium bis[tetrachloroferrate(iii)] chloride molecular magnet: a broken symmetry-DFT study" *Phys. Chem. Chem. Phys.* **17** 19119 (2015).
[19] Baniasadi, F., Tehranchi, M. M., Fathi, M. B. *et al*. "Room temperature photoinduced magnetism in $[py.H]_3[FeCl_4]_2Cl$" *Mater. Chem. Phys*. **168** (15) 35-41 (2015).
[20] Fathi, M. B., Kamalkhani, N. "The plausible superexchange pathway inside the magnetic molecule tripyridinium bis [tetrachloroferrate (III)] chloride via study of DOS and Mos" *Russian Journal of Physical Chemistry A*, (Accepted for publication).
[21] Frisch, M. J., Trucks, G. W., Schlegel, H. B. *et al.*, "Gaussian 03 (Revision A.1)" *Gaussian: Pittsburgh*, PA (2003).

[22] Schubert, K., Gua, M., Atak, K. *et al.* "The electronic structure and deexcitation pathways of an isolated metalloporphyrin ion resolved by metal L-edge spectroscopy" (Edge Article) *Chem. Sci.*, **12** (11) 3966-3976 (2021) (Advance Article).
[23] O'boyle, N. M., Tenderholt, A. L. and Langner, K. M. "cclib: A library for package-independent computational chemistry algorithms" *J. Comput. Chem.* **29** (5) 839-845 (2008).
[24] Valeur, B. *Molecular Fluorescence: Principles and Applications* Digital Encyclopedia of Applied Physics-Wiley Online Library-VCH (2003).
[25] Atkins, P. W. and de Paula, J. *Physical Chemistry* 9th Ed., W H Freeman and Company (2010).
[26] Atkins, P. W. and Friedman, R. *Molecular quantum mechanics* Oxford University Press (2005).
[27] Klessinger, M., Michl, J. *Excited States and Photochemistry of Organic Molecules* 1st Ed., VCH, New York, (1995).
[28] Haug, H. and Koch, S. W. *Quantum Theory of the Optical and Electronic Properties of Semiconductors* World Scientific Publishing (2000).
[29] Klán, P. and Wirzr, J. *Photochemistry of Organic Compounds: From Concepts to Practice* Wiley (2009).
[30] Wang, X., Li, L., Gong, K. *et al.*, "Modelling air quality during the EXPLORE-YRD campaign – Part I. Model performance evaluation and impacts of meteorological inputs and grid resolutions" *Atmospheric environment*, **246** (1) 118131 (2021).
[31] Dong, Y., Peng, W., Liu, Y. *et al.* "Photochemical origin of reactive radicals and halogenated organic substances in natural waters: A review" *Journal of Hazardous Materials*, **401 (**5) 123884 (2021).
[32] Atkins, P. W. and Friedman, R. *Molecular quantum mechanics* Oxford University Press, Oxford, New York (2005).
[33] Baniasadi, F., Sahraei, N., Fathi, M. B. *et al.* "X-ray characterization of tripyridinium bis[tetrabromidoferrate(III)] bromide asymmetric unit in solution by Debye function analysis" *International Journal of Modern Physics B* **30**(24):1650174 (2016).
[34] Grekhov, A. M., Gun'ko, V. M., Klapchenko, G. M. *et al.* "Calculations of electronic structure and density of states of ideal and disordered silicon clusters" *Theor. Exp. Chem.* **20** (4) 447-451 (1984).

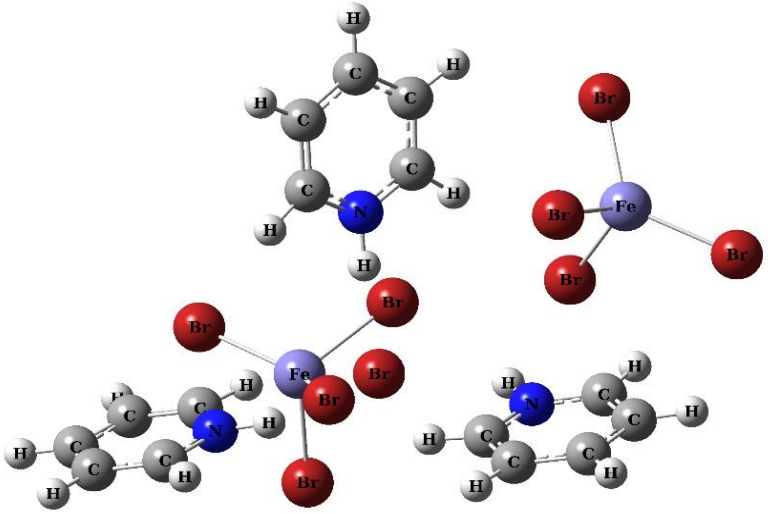

Figure 1 The plausible abundant molecular structure of $[py.H]_3[FeBr_4]_2Br$ complex in acetonitrile [33].

Table 1 Ground state energy of the molecule at different Pople basis sets in atomic units.

Basis Set	Energy	Basis Set	Energy
6-31G	-26418.2737096	6-311G	-26441.1486730
6-31G*	-26419.6481007	6-311G*	-26441.8209699
6-31G**	-26419.6838857	6-311G**	-26441.8565418
6-31+G	-26418.6161250	6-311+G	-26441.2998334
6-31+G*	-26419.8718641	6-311+G*	-26441.8989283
6-31+G**	-26419.9074214	6-311+G**	-26441.9336018
6-31++G	-26418.6254260	6-311++G	-26441.3014524
6-31++G*	-26419.8802820	6-311++G*	-26441.8994215
6-31++G**	-26419.915742	6-311++G**	-26441.9340157

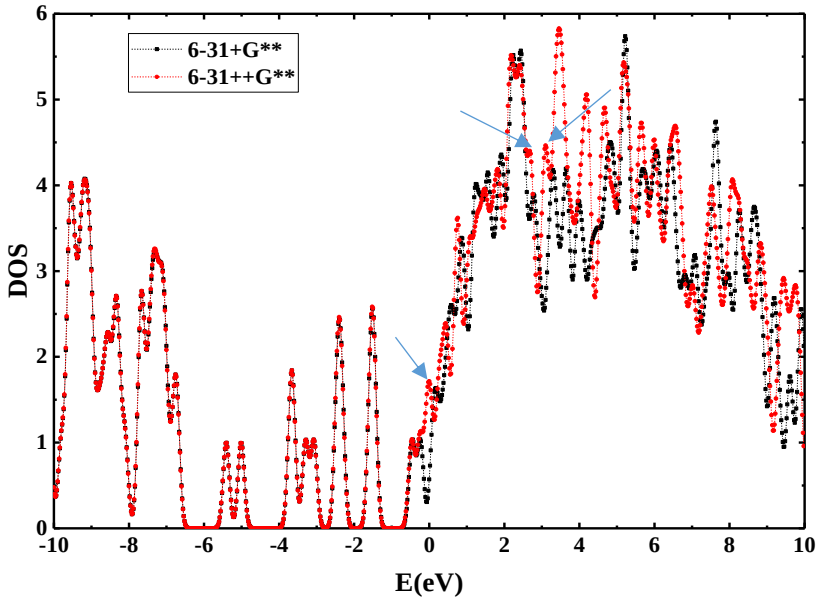

Figure 2 Calculated DOS by Double-zeta Basis Sets: 6-31+G** and 6-31++G**.

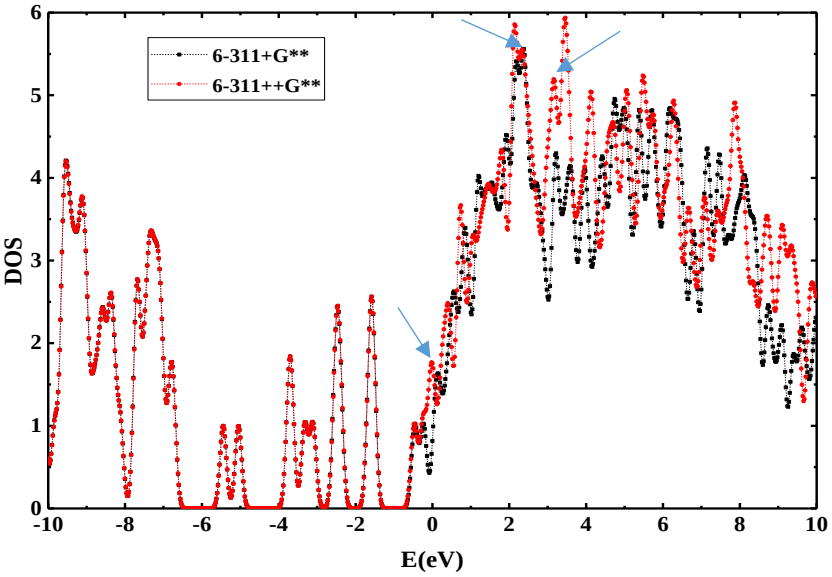

Figure 3 Calculated DOS using Triple-zeta Basis Sets: 6-311+G** and 6-311++G**.

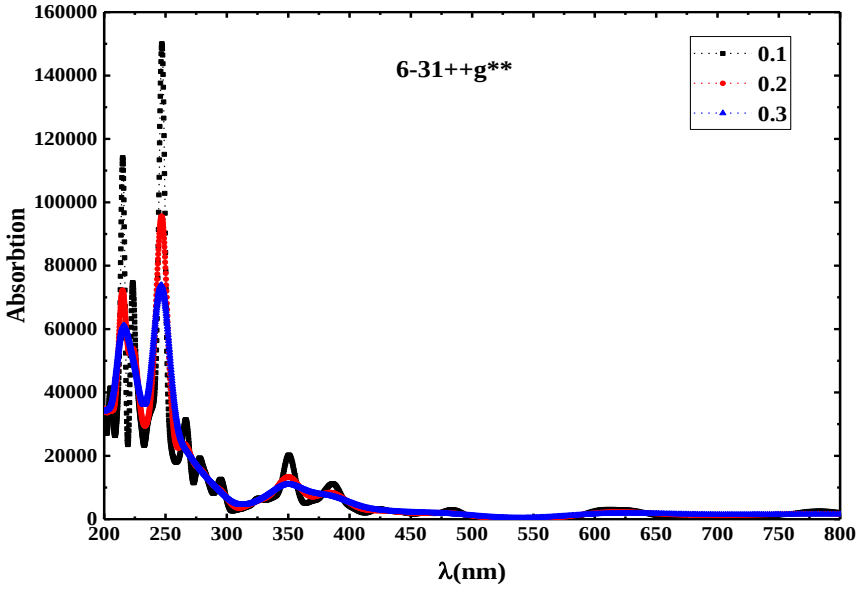

Figure 4 TDDFT simulation of absorption spectra using different FWHM values (0.1, 0.2 and 0.3 eV).

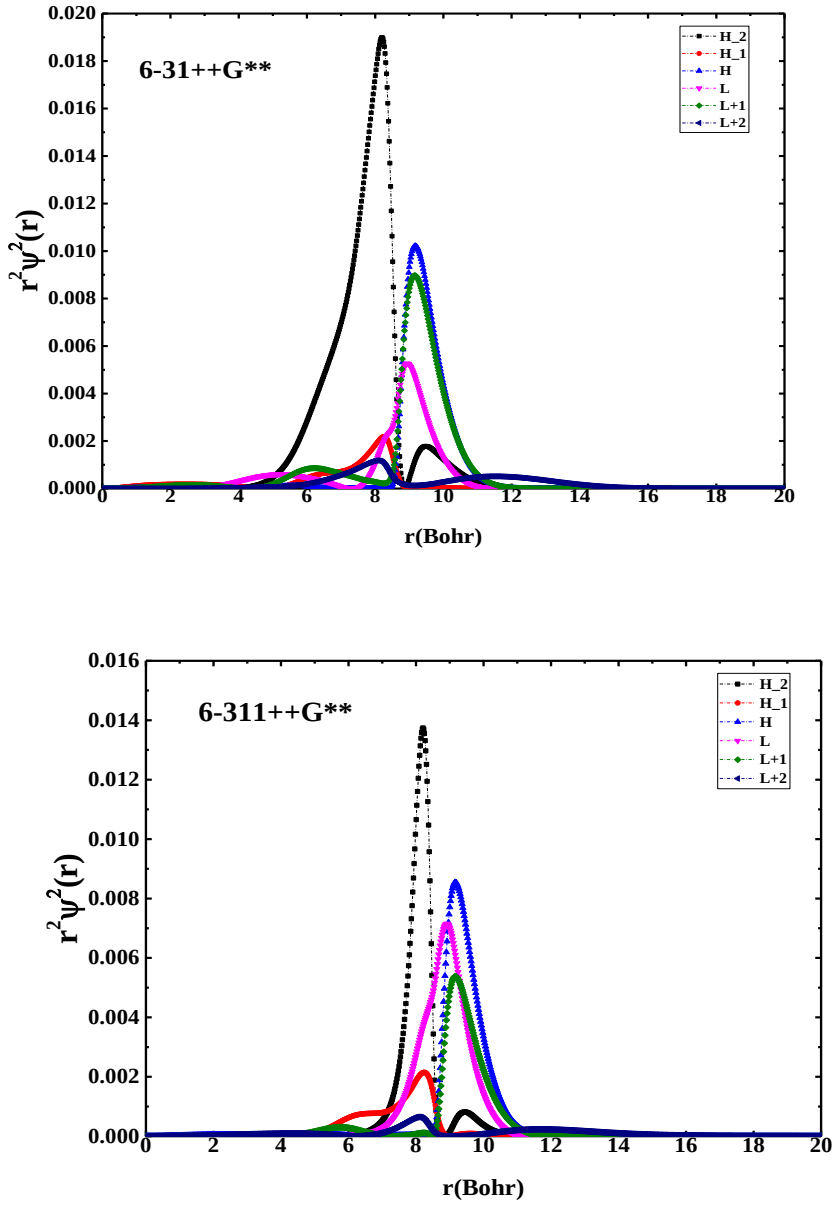

Figure 5 The probability of finding electrons in H-2, H-1, H, L, L+1, L+2.

Table 2 Selected transition dipole matrix elements by 6-31++G** and 6-311++G** basis sets.

Basis set	Transition	E_{ij}(eV)	$\omega_{ij}(\times 10^{15})$	λ(nm)	$p_{nm}(x,y,z)$ / e (Bohr)
6-31++G**	H→L+2	1.78	2.7043	696.54	4.2476×10^{-4}, -8.0085×10^{-3}, 3.6312×10^{-3}
	H→L+1	1.71	2.5979	725.05	1.0050×10^{-2}, -1.1033×10^{-2}, -2.3510×10^{-2}

	H-1 → L	1.7	2.5828	729.32	4.8494×10^{-3}, 5.5148×10^{-2}, -5.2466×10^{-2}
	H-2 → L	1.78	2.7043	696.54	3.7673×10^{-3}, 4.5497×10^{-3}, 4.5060×10^{-3}
6-311++G**	H → L+2	1.78	2.7043	696.54	5.9106×10^{-3}, 9.5928×10^{-3}, -6.3679×10^{-4}
	H → L+1	1.71	2.5979	725.05	-8.0594×10^{-3}, 1.5703×10^{-2}, 1.1932×10^{-2}
	H-1 → L	1.7	2.5828	729.32	-1.2106×10^{-2}, -6.2331×10^{-2}, 6.2424×10^{-2}
	H-2 → L	1.78	2.7043	696.54	-0.1092, -0.1468, 0.1835

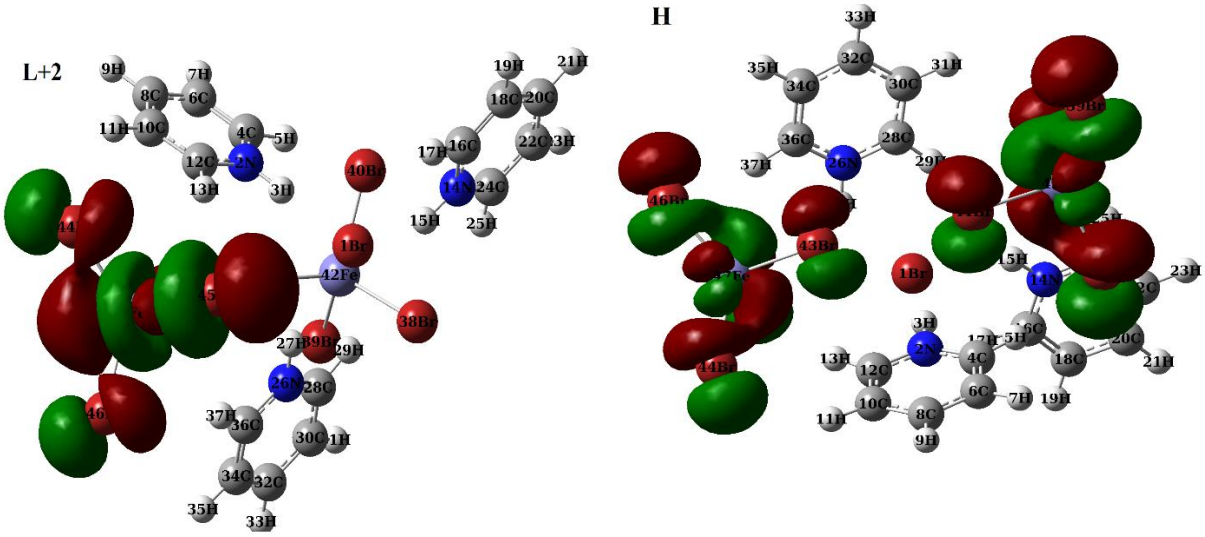

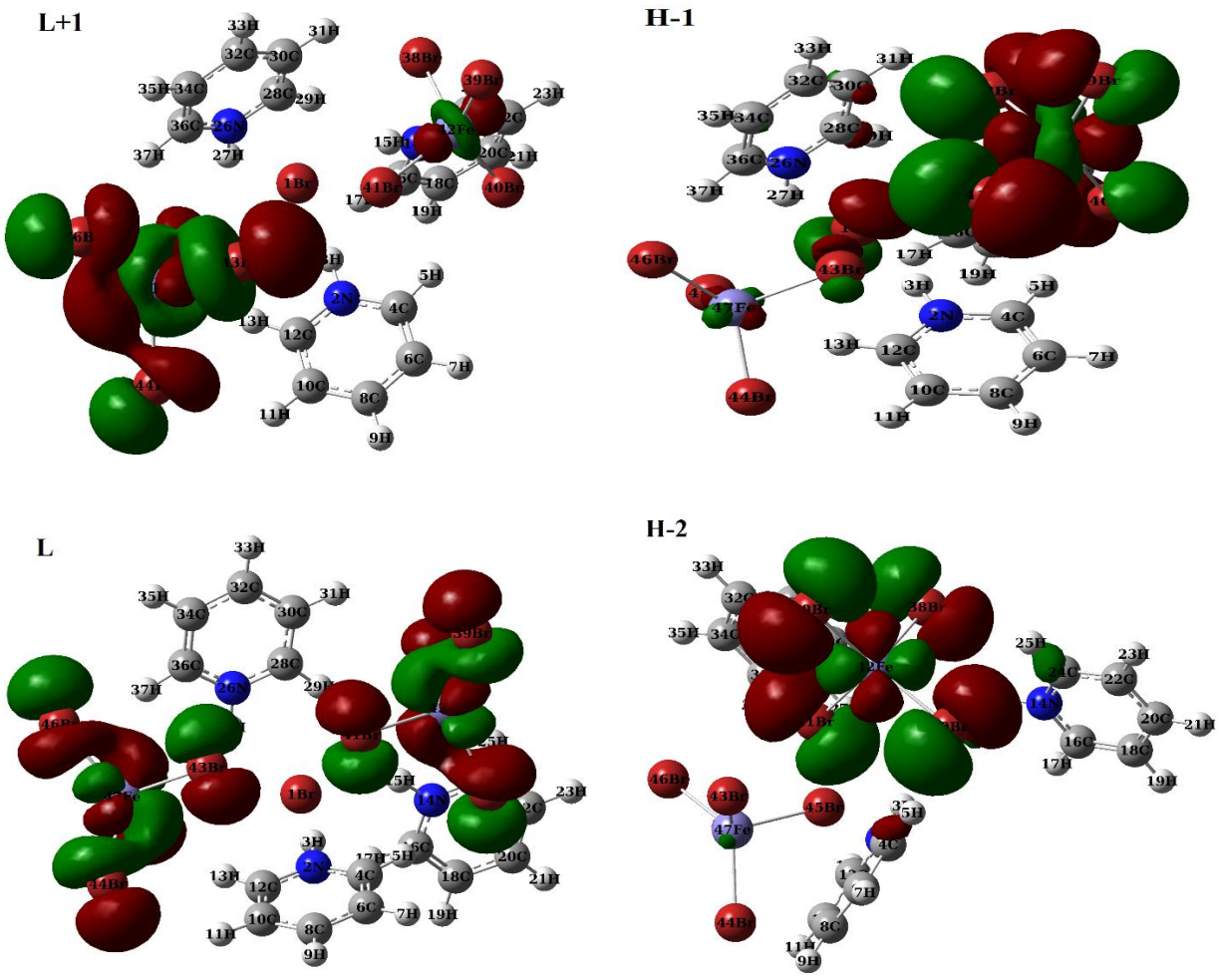

Figure 6 Selected HOMO and LUMOs using 6-31++G** .

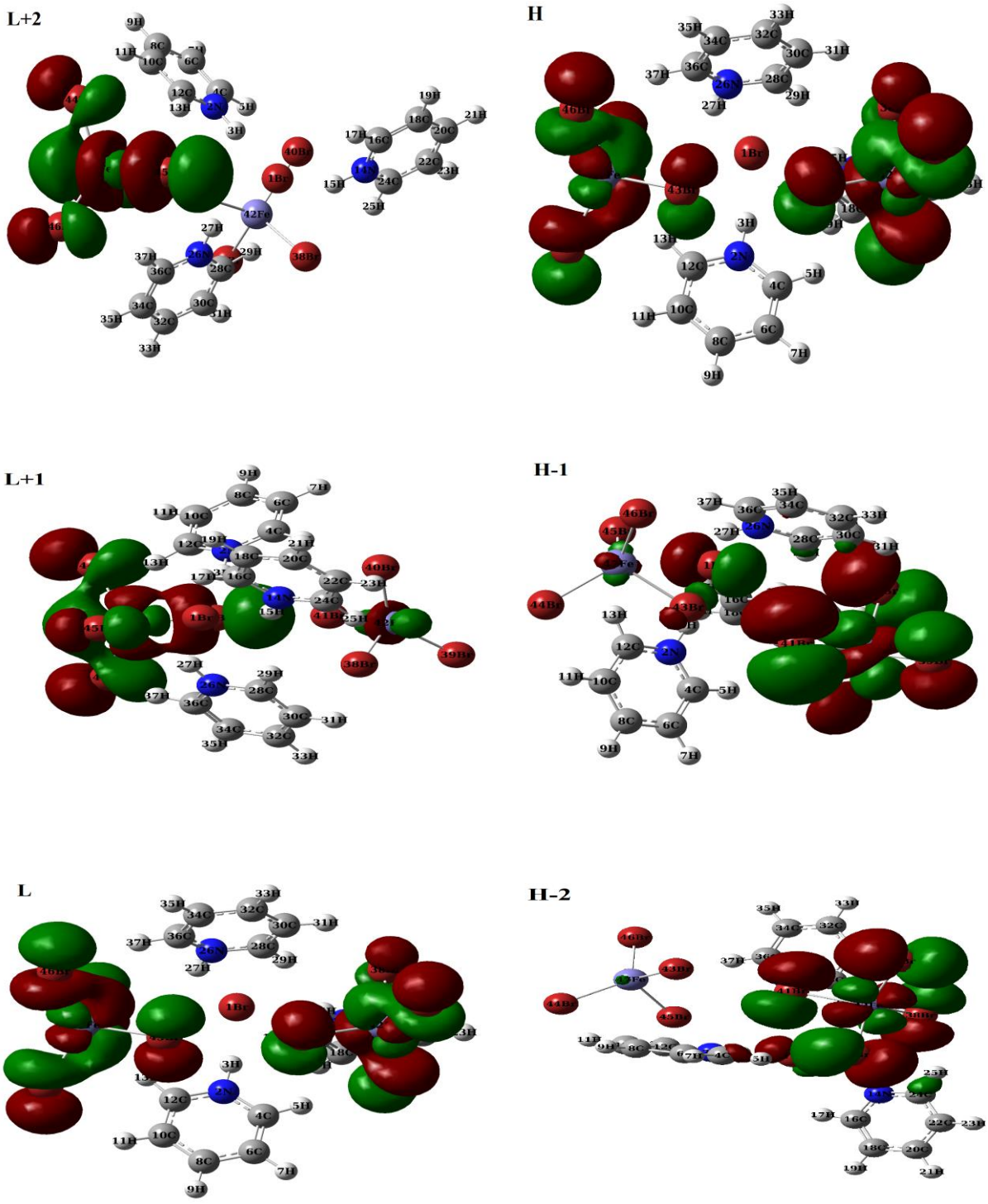

Figure 7 Selected HOMO and LUMOs using 6-311++G**.

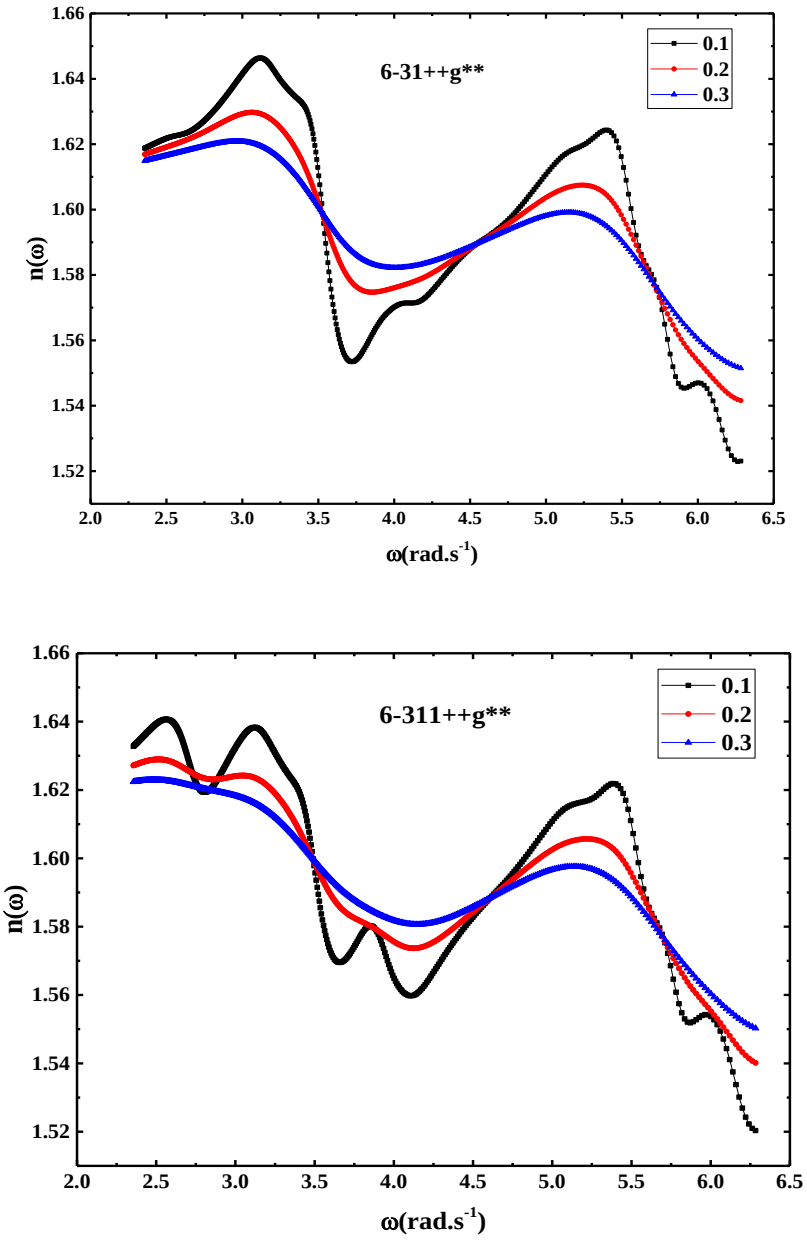

Figure 8 The refractive indexes at the different line-widths (0.1. 0.2 and 0.3 eV).

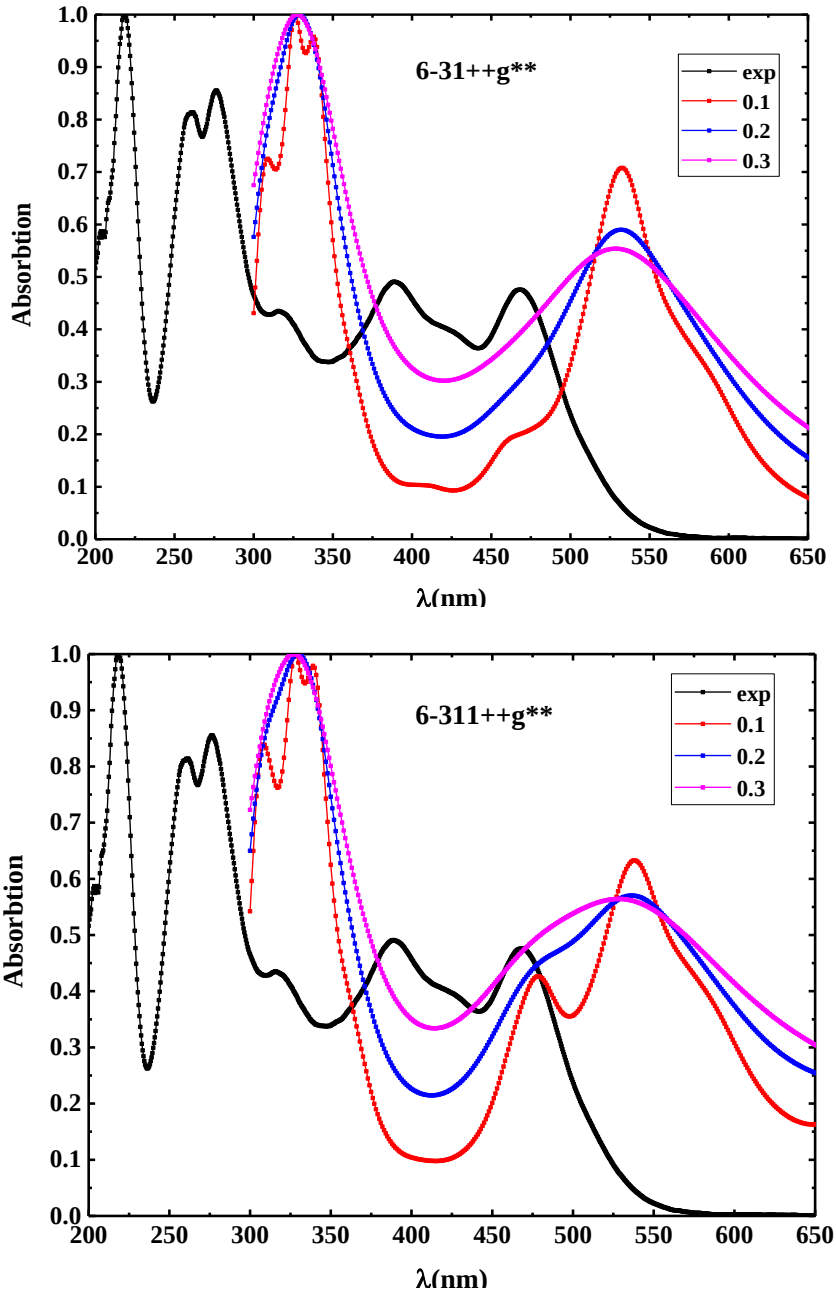

Figure 9 DFT simulation of absorption spectra at different line-widths (0.1. 0.2 and 0.3 eV) are compared with that of experiment.

Dr Farzaneh Baniasadi was born in 1983 in Tehran and graduated from Shahid Beheshti University in December 2015 in the field of quantum physical chemistry under supervision of Professor Mohamad Mehdi Tehranchi and Mohammad Bagher Fathi. Her PhD thesis involved in "photomagnetism" as entitled "Mechanism of photo induced magnetism in [py.H]3[FeCl4]2Cl at room temperature". Study of nanoparticle by optical and statistical method, material simulation and characterization, density functional theory calculation and quantum optical theory was the main scientific topic during Baniasadi's advanced educational (MSc & PhD) courses. After PhD, Farzaneh being involved to Royan institute. Now she is a researcher in Royan institute (cryobiology team) and studying on synthesis of nanoparticles and nontoxicity effect of them on reproduction and cryopreservation. So, she hopes to obtain a green nanoparticle to reduce cryopreservation side effect. Dr Farzaneh Baniasadi published over 7 national and international papers and presented about 10 scientific abstracts and lectures in symposia and congresses.

Dr. M. B. Fathi*

Department of Solid State, Faculty of Physics, Kharazmi University, Tehran, Iran.

He was born in Tehran, Iran. He obtained his B.Sc. in Physics from Shahid Beheshti University in 2002, M.Sc. in Condensed Matter Physics from Shahid Beheshti University in 2004 and PhD in Condensed Matter Physics from Sharif University of Technology in 2010. He is working on different aspects of condensed matter theory from elementary excitations through characterization of materials. His main areas of interests are characterization of strongly correlated materials, especially during phase transitions. He has published many research articles in the national and international journals.

Dr. Vahid Amani received his PhD in inorganic chemistry in 2012 from Shahid Beheshti University. He worked as a postdoctoral researcher at the Department of Chemistry, University of Shahid Beheshti (2012–2015). He was a high school chemistry teacher in Chahardangeh region for 16 years. In 2016, He joined the Department of Chemistry, Farhangian University in Tehran. His research interest lies in coordination chemistry, biochemistry and chemical education. He has authored and co-authored over 230 peer-reviewed research papers.

Porf. M. M. Tehranchi is an Iranian theoretical physicist, distinguished professor at laser and plasma research institute and department of physics of Shahid Beheshti University and member of board of trustees and president of the Islamic Azad University. He was former rector of the Islamic Azad University Central Tehran Branch and Islamic Azad University of Tehran Province and Shahid Beheshti University.